Published in final edited form as:
Cell Stem Cell. 2011 March 4; 8(3): 326–334. doi:10.1016/j.stem.2011.01.001.

FGF2 Sustains *NANOG* and Switches the Outcome of BMP4 Induced Human Embryonic Stem Cell Differentiation

Pengzhi Yu[1,2,3], **Guangjin Pan**[1,*], **Junying Yu**[4], and **James A. Thomson**[1,2,5]

[1]Morgridge Institute for Research, Madison, WI 53707-7365, USA

[2]Cell & Regenerative Biology, University of Wisconsin School of Medicine and Public Health, Madison, WI 53707-7365, USA

[3]Graduate Program in Cellular & Molecular Biology, University of Wisconsin, Madison, WI 53706-1580, USA

[4]Cellular Dynamics International, Inc., Madison, WI 53707-1018, USA

[5]Department of Molecular, Cellular, & Developmental Biology, University of California Santa Barbara, Santa Barbara, CA 93106, USA.

SUMMARY

Here we show that as human embryonic stem (ES) cells exit the pluripotent state, *NANOG* can play a key role in determining lineage outcome. It has previously been reported that BMPs induce differentiation of human ES cells into extraembryonic lineages. Here we find that FGF2, acting through the MEK-ERK pathway, switches BMP4 induced human ES cell differentiation outcome to mesendoderm, characterized by the uniform expression of *T* (brachyury) and other primitive streak markers. We also find that MEK-ERK signaling prolongs *NANOG* expression during BMP-induced differentiation; that forced *NANOG* expression results in FGF independent BMP4 induction of mesendoderm; and that knockdown of *NANOG* greatly reduces *T* induction. Together, our results demonstrate that FGF2 signaling switches the outcome of BMP4 induced differentiation of human ES cells by maintaining *NANOG* levels through the MEKERK pathway.

INTRODUCTION

At day 14 in the human embryo, epiblast cells begin to migrate inward through the primitive streak to form mesoderm and endoderm, marking the start of gastrulation. The term presumptive mesendoderm is sometimes used to describe this early migrating population of cells, as they are thought to contribute to either the mesodermal or endodermal germ layer. Studies from zebrafish embryonic development (Rodaway et al., 1999) and mouse embryonic stem (ES) cells (Gouon-Evans et al., 2006) support this idea. NODAL, BMP,

Correspondence: jthomson@morgridgeinstitute.org.
*Current affiliation: Guangzhou Institutes of Biomedicine and Health, Chinese Academy of Sciences, China

The authors do not declare competing financial interests.

The microarray data are available in the Gene Expression Omnibus (GEO) database (http://www.ncbi.nlm.nih.gov/geo) under the accession number GSE25973.

WNT and FGF signaling pathways, and transcription factors *T, MIXL1, LHX1, and EOMES*, are all involved in primitive streak development (Tam and Loebel, 2007). For example, both *Xenopus* and mouse studies have demonstrated a critical role for BMP signaling in mesoderm formation and dorsal-ventral patterning (Jones et al., 1996; Winnier et al., 1995). However, in human ES cell and mouse epiblast stem cell studies, BMP4 has been shown to induce extraembryonic lineage differentiation (Brons et al., 2007; Xu et al., 2002). The outcome of BMP signaling is context dependent, but exactly why BMP signaling induces extraembryonic lineage in one context and mesoderm in another has not been previously explained.

T (*brachyury homolog*) is a transcription factor expressed in the nascent mesendoderm and is required for primitive streak development (Wilkinson et al., 1990). *T* was first identified from a mouse strain in which heterozygous carriers exhibit a short tail (brachyury) phenotype (Dobrovolskaia-Zavadskaia, 1927). In mice homozygous null for *T*, severe abnormalities are observed from about day 8 of gestation, and death occurs by day 10 of gestation (Chesley, 1935). The abnormalities observed result from a lack of cells migrating through the primitive streak, leading to reduced mesoderm (Yanagisawa et al., 1981). Experiments in *Xenopus* have shown that injecting FGF2 into the animal cap induces primitive streak formation and *Xbra* (a *T* homologue) expression (Smith et al., 1991), and that activation of MAP kinases is required for *Xbra* induction (Umbhauer et al., 1995). It is also been shown that overexpression of *Xbra* in *Xenopus* is sufficient to drive mesendoderm formation (Cunliffe and Smith, 1992). Exactly how MAP kinase activation is linked to *Xbra* induction and primitive streak formation in *Xenopus* is unclear.

In contrast, FGF2 promotes self-renewal of human ES cells (Xu et al., 2005), though the downstream effectors of FGF2 signaling responsible for this are not clearly defined. This is partly due to the complexity of the pathways influenced by FGF signaling, and the varying culture conditions employed by different laboratories. The majority of the FGF downstream effectors are expressed in human ES cells at the mRNA level, and the PI3K-AKT and MEKERK downstream pathways are reportedly active and important for human ES cell self-renewal (Armstrong et al., 2006; Kang et al., 2005). How these downstream FGF pathways intersect with the transcriptional regulators of self-renewal and pluripotency is largely unknown, though blocking FGF signaling causes *NANOG* expression level to decline rapidly (Greber et al., 2010; Xu et al., 2008).

Nanog was first identified in mouse ES cells as a pluripotency-maintaining factor (Chambers et al., 2003; Mitsui et al., 2003), and more recent work has demonstrated the importance of *Nanog* in the acquisition of pluripotency (Silva et al., 2009). Human *NANOG* is part of a core transcriptional regulatory network in ES cells (Boyer et al., 2005), and is capable of enhancing the frequency of molecular reprogramming of human somatic cells into pluripotent cells (Yu et al., 2007). *NANOG* downregulation by RNA interference in human ES cells leads to extra-embryonic lineage differentiation in serum containing medium (Hyslop et al., 2005), and to upregulation of certain neuronal marker genes in a chemically defined medium with ACTIVIN A and FGF2 supplements (Vallier et al., 2009). Forced expression of *NANOG* enables a feeder independent culture of human ES cells (Darr et al., 2006). All of these studies support the idea that *NANOG* plays a central role in acquiring and maintaining pluripotency. Here we show that FGF maintenance of *NANOG* levels during BMP-induced differentiation of human ES cells switches lineage outcome to mesendoderm.

RESULTS

FGF2 switches the outcome of BMP4 induced differentiation of human ES cells

We previously reported that in mouse embryonic fibroblast (MEF) conditioned medium, BMP4 induced differentiation of human ES cells to an extraembryonic tissue enriched for trophoblast specific genes (Xu et al., 2002). However, in defined mTeSR medium (Ludwig et al., 2006a), we did not detect expression of hCG or other trophoblast-specific markers after BMP4 addition. Utilizing whole genome expression microarray analysis, we found that removal of FGF2 from mTeSR, caused upregulation of hCG genes (*CGB*, *CGB5* and *CGA*) by day 5 of BMP4 treatment; the resulting cells were very similar to those previously described in conditioned medium. However, with FGF2 present in mTeSR, BMP4 resulted in the upregulation of primitive streak (*T*, *MIXL1*, *LHX1*, *WNT3*), endoderm (*SOX17*, *CXCR4*) and mesoderm (*TWIST1*, *FOXF1*) marker genes, but not hCG or other trophoblast specific genes (Figure 1A). *FOXA2* transcripts were undetectable and only weak expression of *GSC* was observed in the +FGF2+BMP4 treated cells, which is more characteristic of posterior streak cells. Upregulation of ectoderm-specific genes was undetectable in either condition.

To investigate the timing of differentiation, we performed two time course experiments with either high (50 ng/mL) or low (5 ng/mL) BMP4 in the presence or absence of FGF2 (Figure 1B; Figure S1A, B and C). In both cases, hCG expression was detected after 96 hours in the −FGF2+BMP4 group, while primitive streak gene expression was detected after 18 hours in the +FGF2+BMP4 group. Most endoderm and mesoderm genes were upregulated subsequent to the rise of primitive streak genes. Low-levels of *T* mRNA detected in the -FGF2 with low BMP4 group were likely due to endogenous FGF2 signaling, as an FGF receptor inhibitor (PD173074) abolished detectable *T* expression (Figure 1C) in similar conditions. Compared to treatment with 50ng/mL of BMP4, 5ng/mL of BMP4 treatment produced a much wider time frame for the expression of primitive streak marker genes. Thus we used 5ng/mL of BMP4 to induce differentiation for subsequent experiments. 25ng/mL or higher doses of FGF2 did not show significant differences in maintaining the expression level of *NANOG* or in inducing *T* expression after 36h of BMP4 addition (Figure S1D). Since standard mTeSR medium contains 100ng/mL of FGF2 (Ludwig et al., 2006a), we maintained that concentration for the experiments in this study.

In order to determine the percentage of individual cells expressing T protein, we performed immunostaining and flow cytometry. Immunostaining data showed that T protein was present in the nucleus of most cells after 48 hours of +FGF2+BMP4 treatment (Figure 1D). Few T-positive cells were present after −FGF2+BMP4 treatment, even though endogenous FGF signaling was not blocked in these experiments. Flow cytometry confirmed a uniform shift to increased T expression from the −FGF2+BMP4 to +FGF2+BMP4 treatments (Figure 1E). It should be noted that because the IgG for intracellular staining consistently demonstrated lower signal intensity compared to that of the anti-T antibody in all cells tested, including undifferentiated human ES cells, Figure 1E cannot exclude some low T expression in the -FGF2+BMP4 treated cells. Western blot data confirmed that T protein was not detected from the −FGF2+BMP4 treated cells (Figure S1E). These results show that treatment of human ES cells in defined conditions with BMP4 and high concentrations of FGF2 results in a uniform differentiation of cells expressing the mesendoderm marker *T*.

MEK-ERK pathway is essential for mesendoderm differentiation

In each of the time points examined before the onset of T expression, *DUSP6* was consistently upregulated in the +FGF2+BMP4 treated cells compared to the −FGF2+BMP4 treated cells (Table S1). *DUSP6*, also known as *MKP3*, encodes a cytoplasmic phosphatase

that dephosphorylates and inactivates ERK1/2, but not ERK5 (Arkell et al., 2008). *Dusp6* null mice are viable and have a higher basal phosphorylation of ERK1/2 with unchanged levels of phosphorylation of ERK5, p38, or JNK (Maillet et al., 2008). *DUSP6* expression is induced by phosphorylated ERK1/2, and functions in a negative feedback loop regulating ERK activity (Li et al., 2007). Thus, increased *DUSP6* expression is a reliable indicator of ERK1/2 activity in response to FGF signaling.

To test whether the inactivation of ERK1/2 blocks *T* induction, we overexpressed *DUSP6* in human ES cells, while using *DUSP10* overexpression as a control. *DUSP10* (also known as *MKP5*) encodes a structurally related phosphatase that dephosphorylates p38 and JNK, but not ERK1/2 (Tanoue et al., 1999; Theodosiou et al., 1999). Transgene expression was confirmed by quantitative RT-PCR (Figure 2A). Western blot detecting phosphorylated ERK confirmed that overexpressed DUSP6 was functional. Although significantly reduced, ERK phosphorylation is not completely blocked by *DUSP6* overexpression (Figure 2B). *DUSP6* overexpression suppressed *T* induction in +FGF2+BMP4 treated human ES cells, whereas *DUSP10* overexpression had no effect (Figure 2C). Flow cytometry data (Figure 2D) confirmed that at the protein level, *DUSP6* overexpression reduced *T* induction. Because ERK1/2 are the targets of DUSP6 dephosphorylation, these data suggest that ERK1/2 are key components of the FGF-mediated switch to mesendoderm differentiation.

To verify the importance of ERK1/2 in mesendoderm induction, we added chemical inhibitors against different pathways downstream of FGF signaling to +FGF2+BMP4 treated human ES cells (Figure 2E, F; Figure S2). U0126 (a MEK1/2 inhibitor) and PD173074 (an FGF receptor inhibitor) completely blocked *T* induction, while inhibitors of other downstream pathways (GF109203X against PKC, SP600125 against JNK, LY294002 against PI3K, and SB203580 against p38) had no effect. Also, we induced the expression of a constitutively activated *MEK1*(*MAP2K1*) mutant in H9 cells in the −FGF2+BMP4 condition and found significant *T* upregulation by real time quantitative PCR compared to the wild type *MAP2K1* control and *EGFP* control (Figure 2G). Together, these findings demonstrate that the MEK-ERK pathway is essential for the FGF-mediated switch in BMP4 induced differentiation.

FGF2 prolongs *NANOG* expression during BMP4 treatment resulting in mesendoderm differentiation

In examining the time course of *POU5F1, SOX2,* and *NANOG* expression during -FGF2+BMP4 and +FGF2+BMP4 treatments, we noticed that though the timing of *SOX2* downregulation was similar in the presence or absence of FGF2. *NANOG* or *POU5F1* downregulation was delayed considerably with FGF2 present (Figure 1B; Figure S1C). Downregulation of *POU5F1* did not begin until the maximum induction of *T*, even in the absence of FGF2, suggesting that *POU5F1* is unlikely to contribute to the FGF2 switch. Further, although *NANOG* expression was prolonged in the presence of FGF2, transcript levels eventually decreased, closely paralleling the downregulation of *T*. When ERK activity was suppressed by *DUSP6* overexpression during BMP4 treatment, or when MEK was inactivated by the U0126 inhibitor, FGF2 did not prolong *NANOG* expression, (Figure S3A, B), suggesting that maintenance of *NANOG* by FGF2 requires ERK.

Considering the temporal relationship between *T* and *NANOG* during BMP4 treatment, we hypothesized that the maintenance of *NANOG* by FGF signaling was directly related to the induction and eventual downregulation of *T*. To test this, we used lentiviral vectors to express *NANOG* constitutively in human ES cells followed by treatment with +FGF2+BMP4 and −FGF2+BMP4. These conditions resulted in *T* induction, even in the absence of FGF2 (Figure 3A, B). In addition, we found that expression of *T* was prolonged in cells over-expressing *NANOG*. Although *T* expression normally peaked at 36-48h at the

mRNA level (48-72h at the protein level) and then declined, in cells constitutively expressing *NANOG, T* was still elevated at 5 days (Figure 3C). Western blot data revealed that the total NANOG protein level was not increased by lentiviral overexpression (Figure S3C). Instead, the overall NANOG protein was maintained around the same level even under the −FGF2+BMP4 condition where it would normally be significantly reduced. Since long term *NANOG* knockdown reportedly induces extra-embryonic lineage differentiation, we simultaneously introduced *NANOG* siRNA and treated cells with BMP4 to investigate the short-term effect of *NANOG* knockdown on *T* expression. Compared to control cells after 36h of treatment, *NANOG* siRNA treated cells lost around 80% of endogenous *NANOG* mRNA and had significantly less *T* induction from +FGF2+BMP4 condition (Figure 3D). The knockdown data showed that *NANOG* contributes to successful *T* induction. Taken together, our results suggest that *NANOG* is a critical downstream target of FGF signaling responsible for switching BMP4 induced differentiation of human ES cells to mesendoderm.

DISCUSSION

This study suggests that *NANOG*, in addition to its role in the initiation and maintenance of pluripotency, is involved in mesendoderm specification. Unlike the inner cell mass, later expression of *Nanog* in the primitive ectoderm is nonuniform. *In situ* hybridization data demonstrates that high *Nanog* expression in the egg cylinder stage mouse embryo is restricted to the site of the presumptive streak, and is later restricted to the region of the streak itself (Hart et al., 2004). As cells migrate through the streak, *Nanog* is downregulated. It was therefore suggested that *Nanog*'s highly restricted expression pattern is consistent with a role in pattern formation. Because *Nanog* null embryos lack epiblast, the involvement of *Nanog* in later primitive streak formation could not be examined in those null embryos (Mitsui et al., 2003).

More recently, *Nanog* null mouse ES cells have been successfully generated and, unexpectedly, these ES cells propagated for long periods, and contributed to all three germ layers in chimeras (Chambers et al., 2007). If *Nanog*'s role is conserved in mouse and human development – and this is not yet clear – these results suggest that there is not an absolute requirement for *Nanog* for the induction of primitive streak genes. In this context, results from our work and earlier mouse ES works are more consistent with a protective effect of *Nanog*, where *Nanog* prevents pluripotent stage cells from responding to spurious signals that would otherwise induce them to inappropriate lineages. In our case, it is not clear why BMP signaling induces the expression of trophoblast genes in human ES cells that otherwise appear epiblast-like, as epiblast cells in the mouse do not contribute to trophoblast. It is possible that trophoblast differentiation in our experiments reflects real species-specific differences in lineage specification, but it is also possible that it represents an *in vitro* effect in response to a non-physiological signaling context. Our results may then simply reflect a wider role for *NANOG* in buffering against signaling noise that would otherwise result in inappropriate differentiation outcomes.

Our results demonstrated a positive effect of *NANOG* on *T* expression, but the mechanism connecting the two remains unknown. Preliminary ChIP-seq data failed to detect significant NANOG binding in the T locus region and ChIP-PCR data (Figure S3E) did not show significant binding at a published putative NANOG binding site 4.6kb upstream of the transcriptional starting site of *T* (Boyer et al., 2005). This suggests that *NANOG* may not directly regulate *T* expression. Our findings seem to differ from a previous mouse ES cell study, which suggests that by binding to Smad1, Nanog blocks *T* induction from BMP signaling (Suzuki et al., 2006). However, mouse and human ES cells respond differently to BMP signaling since BMPs promote the self-renewal of mouse ES cells (Ying et al., 2003)

but induce differentiation of human ES cells. These apparent species differences might be related to the differences between the two cell states, as it is currently thought that mouse ES cells closely resemble inner cell mass cells, but human ES cells more closely resemble epiblast cells (Brons et al., 2007; Tesar et al., 2007). In addition, the blocking effect of *Nanog* on *T* in the Suzuki study was supported by a luciferase assay based on 396 bp and 204 bp regions upstream of the mouse *T* promoter. These regions may not include regulatory elements further upstream that might be used differently in inner cell mass versus epiblast cells.

Short-term BMP treatment was also reported to induce mesoderm differentiation of human ES cells (Zhang et al., 2008). Although no exogenous FGF was used in that study, differentiation was induced from human ES cells cultured in MEF conditioned medium, which could act as a source of a variety of growth factors including FGF. This could explain the requirement for only short-term BMP exposure, as it is possible that the endogenous FGF was not enough to sustain NANOG and a mesodermal fate with longer exposure.

Precisely how the MEK-ERK pathway regulates *NANOG* expression remains unknown. A candidate link from MEK-ERK to *NANOG* might be SMAD2/3, as recent reports suggested direct regulation of *NANOG* by SMAD2/3 binding on the promoter region (Greber et al., 2008; Vallier et al., 2009; Xu et al., 2008). Both SMAD2/3 and SMAD1/5/8 pathways were reportedly required for mesendoderm differentiation and FGF2 appeared to sustain SMAD2/3 activating TGFβ ligand expression (Greber et al., 2008). Consistent with their findings, our data showed that mesendoderm differentiation was inhibited in +FGF2+BMP4 condition when SMAD2/3 pathway was blocked by SB431542 (Figure S1I) and that *NODAL* expression was better maintained in the presence of FGF2 during BMP4 induced differentiation (Figure S1A and B). Also, the MEK-ERK pathway is capable of modulating SMAD signaling through phosphorylation of the linker region of various SMAD proteins (Kretzschmar et al., 1997; Matsuura et al., 2005). However, the link between MEK-ERK and *NANOG* expression might be indirect. For example, the dominant early phenotypic effect on undifferentiated human ES cells of FGF2 withdrawal is a slowed proliferation (Ludwig et al., 2006b). So it is possible that the level of *NANOG* is related to cell cycle progression. A causal link between cell cycle progression and *NANOG* expression is unfortunately difficult to test, as cell cycle inhibitors generally result in the apoptosis of human ES cells.

In conclusion, we demonstrate that a mesendodermal outcome of BMP4 induced human ES cell differentiation depends on FGF signaling; that MEK-ERK is the relevant downstream pathway involved; and that *NANOG* is a key transcription factor responsible for determining this outcome in our culture conditions. These findings are particularly important as it demonstrates that *NANOG* is not only involved in the establishment and maintenance of pluripotency, but can serve a role in determining lineage outcome as cells exit the pluripotent state.

EXPERIMENTAL PROCEDURES

Cell culture and reagents

H1, H9 and H14 human ES cells were cultured in mTeSR (Ludwig et al., 2006a) on Matrigel (BD Biosciences, Bedford, MA). Cells were karyotyped using G-banding chromosome analysis prior to experiments. Low passage (<50) ES cells were dissociated by TrypLE (Invitrogen) and seeded at the density of 4×10^4 per cm^2 for all experiments. To induce differentiation, human BMP4 (R&D Systems, Minneapolis, MN) was added from 0h time point when dissociated single cells were plated, and was maintained in medium thereafter.

Lentiviral transduction

The lentiviral vector and packaging of the virus were as described in (Yu et al., 2007). Detailed methods are included in the supplemental material.

Knockdown by siRNA

NANOG ON-TARGETplus SMARTpool siRNA and negative control siRNA were purchased from Dharmacon, Inc. Lafayette, CO. siRNA transfection mixture was prepared according to manufacturer's instructions, and introduced at the same time BMP4 was added to the cell culture. Cells were collected for RNA extraction after 36h of treatment.

Inducible *MAP2K1* expression

Wild type and a constitutively active *MAP2K1* were PCR cloned from plasmids pENTR1A-W1 and pENTR1A-CC2 developed by Dr. Paul A. Khavari's lab (Scholl et al., 2004). Genes were placed under the control of pTight promoter in a vector that contains the rtTA-expressing cassette and a puromycin resistant element. Elements of the doxcycline inducible system were cloned from plasmids purchased from Clontech, Mountain View, CA. Vectors were introduced into EBNA1 expressing H9 cells with the help of FuGene HD (Roche, Indianapolis, IN). 1ng/mL of puromycin was used to select positive cells 2 days after transfection. Surviving cells were individualized with TrypLE and plated into −FGF2+BMP4 medium to initiate differentiation for 48h in the presence or absence of doxycyclin (0.5 μg/mL).

Immunostaining

Adherent cells were washed 3 times with PBS before being fixed in 2% paraformaldehyde for 20 minutes at room temperature, then blocked and permeabilized in PBS with 0.3% Triton X-100, 10% normal horse serum and 1% BSA at room temperature for 30 minutes. Cells were then incubated with 0.2 g/mL of anti-T antibody (R&D systems) in PBS with 0.2% BSA and 0.01% Triton X-100 at 4°C overnight followed by FITC conjugated anti-goat IgG in dark at room temperature for 1 hour. Cells were washed with PBS containing 0.1% BSA and 0.01% Triton X-100 three times between each step. Vectashield mounting medium for fluorescence with DAPI (Vector Laboratories, Burlingame, CA) was added before visualizing and taking photos under the microscope.

Flow cytometry

Cells were individualized by Trypsin-EDTA (Invitrogen), fixed in 2% paraformaldehyde for 20 minutes at room temperature, and permeabilized in 90% methanol at −20°C overnight. Cells were re-suspended in PBS with 2% FBS and 0.1% sodium azide (FACS buffer), later blocked with PBS with 0.3% Triton X-100, and 2% BSA at room temperature for 30 minutes. 0.5 g/mL of anti-T antibody (R&D systems) or goat IgG (Santa Cruz Biotechnology, Santa Cruz, CA) were added in FACS buffer with 0.01% Triton X-100 at 4°C overnight, followed by FITC conjugated anti-goat IgG antibody in dark at room temperature for 1 hour. Between each steps, cells were washed with FACS buffer three times. A PE conjugated anti-T antibody from R&D systems was later used in this study at 1:400 dilutions. Cells were analyzed on a FACSAria flow cytometer (BDIS, San Jose, CA) using FACSDiva Software. Final data were prepared in FlowJo 6.3 software (Tree Star, Ashland, OR).

Supplementary Material

Refer to Web version on PubMed Central for supplementary material.

Acknowledgments

This work was supported by the Charlotte Geyer Foundation and NIH grant PO1 GM081629. We thank Zhonggang Hou for providing the doxycyclin inducible system vector, Shulan Tian and Ron Stewart for their bioinformatics support, Gudrun A. Jonsdottir for performing sample labeling and hybridization in microarray analysis, and Justin Brumbaugh, Deborah J. Faupel and Krista Eastman for critical reading of the manuscript.

REFERENCES

Arkell RS, Dickinson RJ, Squires M, Hayat S, Keyse SM, Cook SJ. DUSP6/MKP-3 inactivates ERK1/2 but fails to bind and inactivate ERK5. Cell Signal 2008;20:836–843. [PubMed: 18280112]

Armstrong L, Hughes O, Yung S, Hyslop L, Stewart R, Wappler I, Peters H, Walter T, Stojkovic P, Evans J, et al. The role of PI3K/AKT, MAPK/ERK and NFkappabeta signalling in the maintenance of human embryonic stem cell pluripotency and viability highlighted by transcriptional profiling and functional analysis. Hum Mol Genet 2006;15:1894–1913. [PubMed: 16644866]

Boyer LA, Lee TI, Cole MF, Johnstone SE, Levine SS, Zucker JP, Guenther MG, Kumar RM, Murray HL, Jenner RG, et al. Core transcriptional regulatory circuitry in human embryonic stem cells. Cell 2005;122:947–956. [PubMed: 16153702]

Brons IG, Smithers LE, Trotter MW, Rugg-Gunn P, Sun B, Chuva de Sousa Lopes SM, Howlett SK, Clarkson A, Ahrlund-Richter L, Pedersen RA, et al. Derivation of pluripotent epiblast stem cells from mammalian embryos. Nature 2007;448:191–195. [PubMed: 17597762]

Chambers I, Colby D, Robertson M, Nichols J, Lee S, Tweedie S, Smith A. Functional expression cloning of Nanog, a pluripotency sustaining factor in embryonic stem cells. Cell 2003;113:643–655. [PubMed: 12787505]

Chambers I, Silva J, Colby D, Nichols J, Nijmeijer B, Robertson M, Vrana J, Jones K, Grotewold L, Smith A. Nanog safeguards pluripotency and mediates germline development. Nature 2007;450:1230–1234. [PubMed: 18097409]

Chesley P. Development of the short-tailed mutant in the house mouse. Journal of Experimental Zoology 1935;70:429–459.

Cunliffe V, Smith JC. Ectopic mesoderm formation in Xenopus embryos caused by widespread expression of a Brachyury homologue. Nature 1992;358:427–430. [PubMed: 1641026]

Darr H, Mayshar Y, Benvenisty N. Overexpression of NANOG in human ES cells enables feeder-free growth while inducing primitive ectoderm features. Development 2006;133:1193–1201. [PubMed: 16501172]

Dobrovolskaia-Zavadskaia N. Sur la mortification sponta-nee de la queue chez la souris nouveau-nee et sur l'existence d'un caractere hereditaire “non viable”. CR Seanc Soc Biol 1927;97:114–116.

Gouon-Evans V, Boussemart L, Gadue P, Nierhoff D, Koehler CI, Kubo A, Shafritz DA, Keller G. BMP-4 is required for hepatic specification of mouse embryonic stem cell-derived definitive endoderm. Nat Biotechnol 2006;24:1402–1411. [PubMed: 17086172]

Greber B, Lehrach H, Adjaye J. Control of early fate decisions in human ES cells by distinct states of TGFbeta pathway activity. Stem Cells Dev 2008;17:1065–1077. [PubMed: 18393632]

Greber B, Wu G, Bernemann C, Joo JY, Han DW, Ko K, Tapia N, Sabour D, Sterneckert J, Tesar P, et al. Conserved and Divergent Roles of FGF Signaling in Mouse Epiblast Stem Cells and Human Embryonic Stem Cells. Cell Stem Cell 2010;6:215–226. [PubMed: 20207225]

Hart AH, Hartley L, Ibrahim M, Robb L. Identification, cloning and expression analysis of the pluripotency promoting Nanog genes in mouse and human. Dev Dyn 2004;230:187–198. [PubMed: 15108323]

Hyslop L, Stojkovic M, Armstrong L, Walter T, Stojkovic P, Przyborski S, Herbert M, Murdoch A, Strachan T, Lako M. Downregulation of NANOG induces differentiation of human embryonic stem cells to extraembryonic lineages. Stem Cells 2005;23:1035–1043. [PubMed: 15983365]

Jones CM, Dale L, Hogan BL, Wright CV, Smith JC. Bone morphogenetic protein-4 (BMP-4) acts during gastrula stages to cause ventralization of Xenopus embryos. Development 1996;122:1545–1554. [PubMed: 8625841]

Kang HB, Kim JS, Kwon HJ, Nam KH, Youn HS, Sok DE, Lee Y. Basic fibroblast growth factor activates ERK and induces c-fos in human embryonic stem cell line MizhES1. Stem Cells Dev 2005;14:395–401. [PubMed: 16137228]

Kretzschmar M, Doody J, Massague J. Opposing BMP and EGF signalling pathways converge on the TGF-beta family mediator Smad1. Nature 1997;389:618–622. [PubMed: 9335504]

Li C, Scott DA, Hatch E, Tian X, Mansour SL. Dusp6 (Mkp3) is a negative feedback regulator of FGF-stimulated ERK signaling during mouse development. Development 2007;134:167–176. [PubMed: 17164422]

Ludwig TE, Bergendahl V, Levenstein ME, Yu J, Probasco MD, Thomson JA. Feeder-independent culture of human embryonic stem cells. Nat Methods 2006a;3:637–646. [PubMed: 16862139]

Ludwig TE, Levenstein ME, Jones JM, Berggren WT, Mitchen ER, Frane JL, Crandall LJ, Daigh CA, Conard KR, Piekarczyk MS, et al. Derivation of human embryonic stem cells in defined conditions. Nat Biotechnol 2006b;24:185–187. [PubMed: 16388305]

Maillet M, Purcell NH, Sargent MA, York AJ, Bueno OF, Molkentin JD. DUSP6 (MKP3) null mice show enhanced ERK1/2 phosphorylation at baseline and increased myocyte proliferation in the heart affecting disease susceptibility. J Biol Chem 2008;283:31246–31255. [PubMed: 18753132]

Matsuura I, Wang G, He D, Liu F. Identification and characterization of ERK MAP kinase phosphorylation sites in Smad3. Biochemistry 2005;44:12546–12553. [PubMed: 16156666]

Mitsui K, Tokuzawa Y, Itoh H, Segawa K, Murakami M, Takahashi K, Maruyama M, Maeda M, Yamanaka S. The homeoprotein Nanog is required for maintenance of pluripotency in mouse epiblast and ES cells. Cell 2003;113:631–642. [PubMed: 12787504]

Rodaway A, Takeda H, Koshida S, Broadbent J, Price B, Smith JC, Patient R, Holder N. Induction of the mesendoderm in the zebrafish germ ring by yolk cell-derived TGF-beta family signals and discrimination of mesoderm and endoderm by FGF. Development 1999;126:3067–3078. [PubMed: 10375499]

Scholl FA, Dumesic PA, Khavari PA. Mek1 alters epidermal growth and differentiation. Cancer Res 2004;64:6035–6040. [PubMed: 15342384]

Silva J, Nichols J, Theunissen TW, Guo G, van Oosten AL, Barrandon O, Wray J, Yamanaka S, Chambers I, Smith A. Nanog is the gateway to the pluripotent ground state. Cell 2009;138:722–737. [PubMed: 19703398]

Smith JC, Price BM, Green JB, Weigel D, Herrmann BG. Expression of a Xenopus homolog of Brachyury (T) is an immediate-early response to mesoderm induction. Cell 1991;67:79–87. [PubMed: 1717160]

Suzuki A, Raya A, Kawakami Y, Morita M, Matsui T, Nakashima K, Gage FH, Rodriguez-Esteban C, Izpisua Belmonte JC. Nanog binds to Smad1 and blocks bone morphogenetic protein-induced differentiation of embryonic stem cells. Proc Natl Acad Sci U S A 2006;103:10294–10299. [PubMed: 16801560]

Tam PP, Loebel DA. Gene function in mouse embryogenesis: get set for gastrulation. Nat Rev Genet 2007;8:368–381. [PubMed: 17387317]

Tanoue T, Moriguchi T, Nishida E. Molecular cloning and characterization of a novel dual specificity phosphatase, MKP-5. J Biol Chem 1999;274:19949–19956. [PubMed: 10391943]

Tesar PJ, Chenoweth JG, Brook FA, Davies TJ, Evans EP, Mack DL, Gardner RL, McKay RD. New cell lines from mouse epiblast share defining features with human embryonic stem cells. Nature 2007;448:196–199. [PubMed: 17597760]

Theodosiou A, Smith A, Gillieron C, Arkinstall S, Ashworth A. MKP5, a new member of the MAP kinase phosphatase family, which selectively dephosphorylates stress-activated kinases. Oncogene 1999;18:6981–6988. [PubMed: 10597297]

Umbhauer M, Marshall CJ, Mason CS, Old RW, Smith JC. Mesoderm induction in Xenopus caused by activation of MAP kinase. Nature 1995;376:58–62. [PubMed: 7541116]

Vallier L, Mendjan S, Brown S, Chng Z, Teo A, Smithers LE, Trotter MW, Cho CH, Martinez A, Rugg-Gunn P, et al. Activin/Nodal signalling maintains pluripotency by controlling Nanog expression. Development 2009;136:1339–1349. [PubMed: 19279133]

Wilkinson DG, Bhatt S, Herrmann BG. Expression pattern of the mouse T gene and its role in mesoderm formation. Nature 1990;343:657–659. [PubMed: 1689462]

Winnier G, Blessing M, Labosky PA, Hogan BL. Bone morphogenetic protein-4 is required for mesoderm formation and patterning in the mouse. Genes Dev 1995;9:2105–2116. [PubMed: 7657163]

Xu RH, Chen X, Li DS, Li R, Addicks GC, Glennon C, Zwaka TP, Thomson JA. BMP4 initiates human embryonic stem cell differentiation to trophoblast. Nat Biotechnol 2002;20:1261–1264. [PubMed: 12426580]

Xu RH, Peck RM, Li DS, Feng X, Ludwig T, Thomson JA. Basic FGF and suppression of BMP signaling sustain undifferentiated proliferation of human ES cells. Nat Methods 2005;2:185–190. [PubMed: 15782187]

Xu RH, Sampsell-Barron TL, Gu F, Root S, Peck RM, Pan G, Yu J, Antosiewicz-Bourget J, Tian S, Stewart R, et al. NANOG is a direct target of TGFbeta/activin-mediated SMAD signaling in human ESCs. Cell Stem Cell 2008;3:196–206. [PubMed: 18682241]

Yanagisawa KO, Fujimoto H, Urushihara H. Effects of the brachyury (T) mutation on morphogenetic movement in the mouse embryo. Dev Biol 1981;87:242–248. [PubMed: 7286429]

Ying QL, Nichols J, Chambers I, Smith A. BMP induction of Id proteins suppresses differentiation and sustains embryonic stem cell self-renewal in collaboration with STAT3. Cell 2003;115:281–292. [PubMed: 14636556]

Yu J, Vodyanik MA, Smuga-Otto K, Antosiewicz-Bourget J, Frane JL, Tian S, Nie J, Jonsdottir GA, Ruotti V, Stewart R, et al. Induced pluripotent stem cell lines derived from human somatic cells. Science 2007;318:1917–1920. [PubMed: 18029452]

Zhang P, Li J, Tan Z, Wang C, Liu T, Chen L, Yong J, Jiang W, Sun X, Du L, et al. Short-term BMP-4 treatment initiates mesoderm induction in human embryonic stem cells. Blood 2008;111:1933–1941. [PubMed: 18042803]

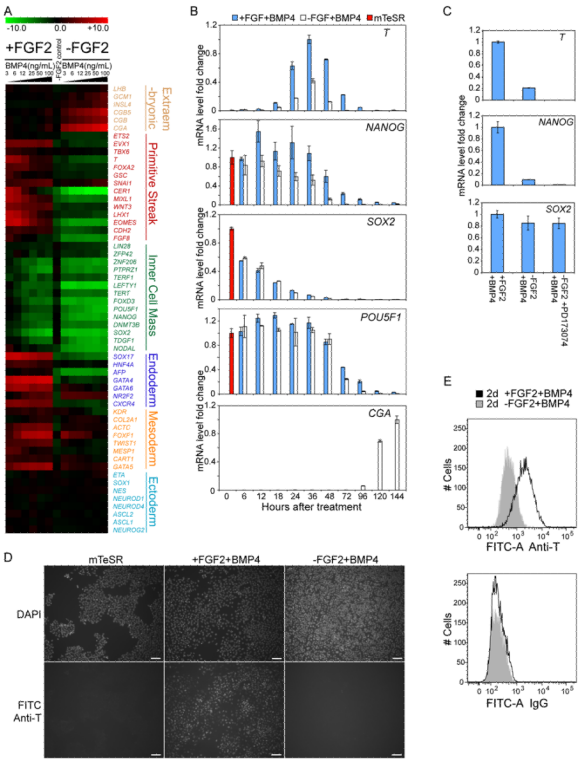

Figure 1. FGF2 signaling switches the outcome of BMP4 induced differentiation of human ES cells

(A) Microarray data showing expression levels of selected lineage marker genes from H1 cells treated with different concentrations of BMP4 for 5 days, w/ or w/o FGF2. Fold change values, shown in $\log_2$ scale, were normalized against data from H1 ES cells grown in mTeSR medium. (B) Expression levels of selected genes during a 5 ng/mL BMP4 time course, detected by quantitative RT-PCR. Error bars represent standard deviations from 3 replicates. mTeSR cultured H1 ES cell control data (red) was set as 1 for each gene except *T*, whose expression level was normalized against data from 36h +FGF2+BMP4 treated cells. (C) FGF receptor inhibitor PD173074 inhibited *T* induction at the 36 h time point shown by quantitative RT-PCR analysis. Average expression level from +FGF2+BMP4 group was set as 1 for each gene. (D) T protein detected by immunostaining. Top row: DAPI nuclei staining; bottom row: FITC channel showing T staining; Scale bar: 0.1mm. (E) Flow cytometry data revealed a uniform shift from −FGF2+BMP4 population (shaded grey) to +FGF2+BMP4 population (solid black) for T staining.

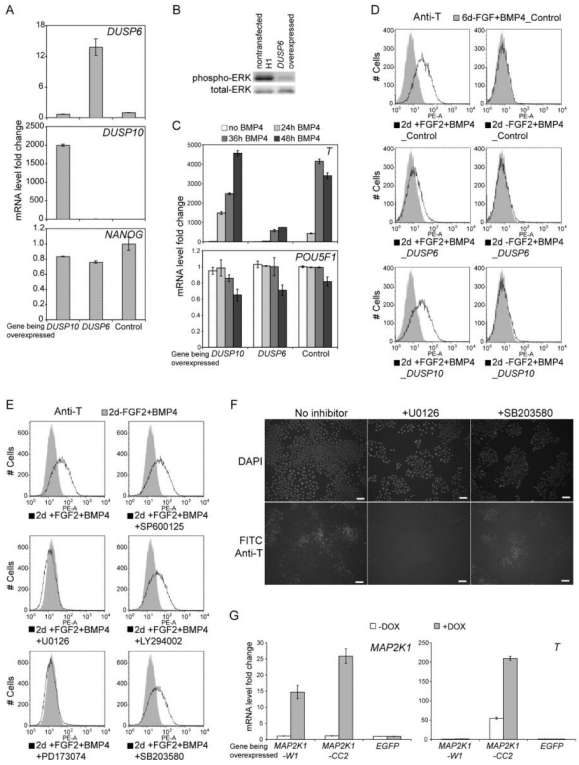

Figure 2. MEK-ERK pathway is required for mesendoderm induction

(A) Quantitative RT-PCR analysis confirmed transgene expression in *DUSP6* and *DUSP10* overexpressing cells. Messenger RNA levels were normalized to that from the non-transfected human ES cells. Error bars represent standard deviations from 3 replicates. (B) *DUSP6* overexpression reduced ERK phosphorylation compared to non-transfected H1 ES cells, detected by western blot. (C and D) *DUSP6* overexpression suppressed the induction of *T* upon +FGF2+BMP4 treatment, confirmed by both quantitative RT-PCR (C), and flow cytometry (D). mRNA levels were normalized to that of the non-treated control cells in (C). (E and F) Flow cytometry and immunostaining for T induction with inhibitors. FGF receptor inhibitor PD173074 and MEK inhibitor U0126 blocked the induction of *T* upon +FGF2+BMP4 treatment, while other inhibitors: SB203580 against p38; SP600125 against JNK; and LY294002 against PI3K, failed to block T induction. Scale bar: 0.1mm, in (F). (G) Only constitutively activated *MEK1* mutant (*MAP2K1-CC*) upregulated *T* expression in the −FGF2+BMP4 conditon compared to wild type *MEK1* (*MAP2K1-W1*) control and *EGFP* control. A single plasimid with doxycycline inducible elements was used to express transgenes in H9 cells. mRNA levels were normalized against that from *EGFP* control in -DOX condition.

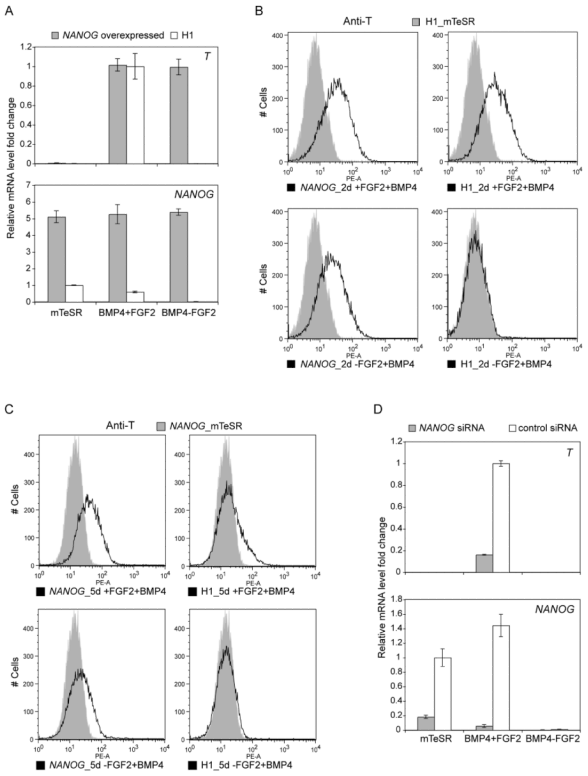

Figure 3. *NANOG* substitutes for the requirement of FGF2 in switching the outcome of BMP4 induced differentiation

(A) *NANOG* constitutively expressed cells induced *T* expression after 36h of −FGF2+BMP4 treatment, detected by quantitative RT-PCR. Error bars represent standard deviations from 3 replicates. mRNA levels of *T* and *NANOG* were normalized against +FGF2+BMP4 treated H1 cells and mTeSR cultured H1 cells respectively. (B) Most *NANOG* overexpressed cells were T positive detected by flow cytometry at 48h of BMP4 treatment in both +FGF2 and −FGF2 groups. Non-treated H1 ES cells served as negative control (shaded grey). The non-transduced ES cell control panel is the same as in Figure 2D, since the data were from the same set of expriment with the same control samples. (C) *NANOG* overexpressing cells had an extended *T* expression time window at day 5 of differentiation. *NANOG* overexpressing cells cultured in mTeSR were included as negative control (shaded grey). (D) *NANOG* knockdown by siRNA reduced *T* expression level at 36h from +FGF2+BMP4 treated cells. siRNAs were introduced at the same time when cells were treated with BMP4. 0.1 μM PD173074 was used to block endogenous FGF signaling in the −FGF2+BMP4 condition in all sub panels in this figure.

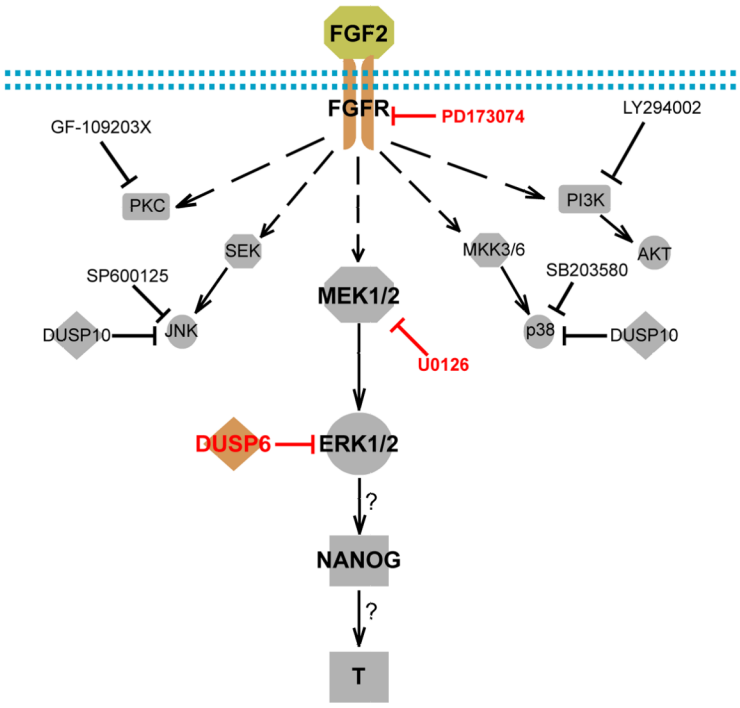

Figure 4. Simplified model for the mechanism of the FGF2 switch on BMP4 induced differentiation outcomes

Arrow represented activation or induction, dashed arrow represented indirect activation with multiple steps involved, hammer-ended line represented inhibition, and arrow with question mark represented induction with mechanism undiscovered. Red labeled inhibitors on the MEK-ERK pathway that blocked *T* induction.